J2J.6 KINEMATIC AND MICROPHYSICAL CHARACTERISTICS OF A STRATIFORM RAIN BAND OBSERVED IN TROPICAL STORM GABRIELLE AT LANDFALL

Dong-Kyun Kim* and Kevin R. Knupp
University of Alabama in Huntsville, Huntsville, Alabama

1. INTRODUCTION

In the recent years, radar wind profilers have been used to study the kinematic and microphysical structures of precipitating storms. Estimation of vertical air motion and horizontal divergence within these systems is important for understanding microphysical and dynamical processes, and verifying numerical models. Wind profilers and scanning Doppler radars can be used as a complement for each other even though they have different scanning techniques and spatial scales (Cifelli et al. 1996). In many studies, the vertical air motion and horizontal divergence fields have been directly derived and analyzed using the single-Doppler radar techniques such as VAD (Browning and Wexler 1968), EVAD (Srivastava et al. 1986; Matejka and Srivastava 1991), and CEVAD (Cifelli et al. 1996). One important assumption for these techniques is that the wind field across the analysis domain is homogeneous and the vertical air motion at the top and bottom boundaries is usually set to zero. Cifelli et al (1996) showed that the vertical profiles of vertical air motion and horizontal divergence derived from scanning radar was in qualitative agreement with those from the wind profiler in the lower atmosphere that showed much more variations of them, however.

In this study, we apply the EVAD technique to the Smart-R radar and the quasi-VAD technique to the 915-wind profiler and analyze the quantities of the wind fields derived from each technique.

2. CASE

On 12 UTC 14 September 2001 tropical storm Gabrielle made landfall along the west coast of Florida. Detailed observations of Gabrielle were made by Mobile Integrated Profiling Systems (MIPS), a SMART-Radar located 1 km east of the MIPS, and the Tampa Bay WSR-88D radar located about 70 km to the north (See Figure 1). The storm moved north and northeastward at a speed of about 6 ms^{-1}. At this direction, the widespread stratiform region swirled with a convective region following it. Winds were southeasterly at the surface and veered with height. The SMART-Radar (5.5 cm wavelength)

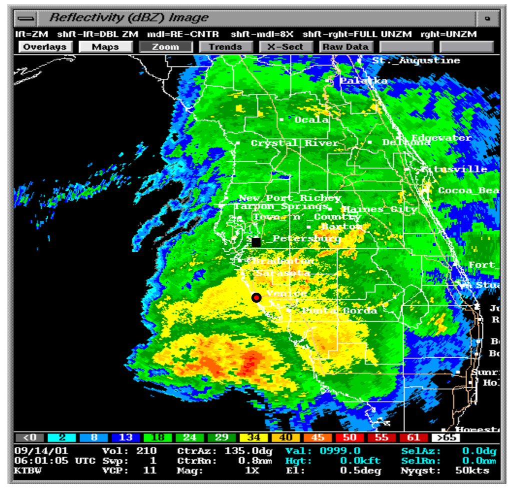

Figure 1. The WSR-88D reflectivity image taken at Tampa on 0601 UTC (0.5°). The red circle and black rectangle show the locations of MIPS/SMART-Radar and the Tampa Bay WSR-88D radar, respectively.

has elevation angles from 1.8° to 44.2° incorporating 17 elevation sweeps over a 5 min period. The 915-wind profiler was operated using five beams; one is vertical and four others are off-vertical 23.6 degree from the zenith. The dwell time on each beam is about 30 sec, and the vertical beam was sampled every 60 sec.

3. METHOD

The VAD (Velocity Azimuth Display) method was first documented by Browning and Wexler (1968). In this study we use the extended VAD (EVAD, Srivastava et al. 1986) for examining profiles of horizontal divergence, vertical air motion and precipitation terminal fall speed. In contrast to VAD, EVAD is not restricted to low elevation angles (in fact, high elevation angles are required) and does not require knowledge of the hydrometeor fall speed. EVAD analyzes a number of horizontal rings in all elevation cones which belong to each layer and yields vertical air motions, vertical target velocity, target terminal fall

*Corresponding author address : Dong-Kyun Kim, National Space Science & Technology Center 320 Sparkman Dr, Huntsville, AL. Email:dkkim@uah.nsstc.edu

speed, and horizontal divergence for the specified depth of each layer. This EVAD technique includes various processes such as Fourier fits, dealiasing velocities, cutting off outliers, and multi-regressions. The Fourier coefficients for the zeroth harmonic (a_0) and first harmonic (a_1 and b_1) determine the divergence and the u and v components of the wind field, respectively. The solutions obtained by repeating the regression for different vertical intervals yield a profile of horizontal divergence and vertical target velocity. The maximum allowable azimuthal gap is 30 degrees (Matejka and Srivastava 1991) but in this work a gap of 36 degrees is set to avoid the effect of beam blockages by the truck cabin and trees at low elevation angles.

Kinematic computations of horizontal divergence and vertical air motion are also performed from the 915 MHz wind profiler measurements. We calculate the gradients of u and v components using two oppositely directed beams. We obtain a profile of vertical air motions by integrating the anelastic continuity equation from top to bottom.

4. RESULTS

Figure 2 shows time-height sections of the Doppler vertical air velocity and the radar reflectivity derived from the 915-MHz profiler using the radar equation. The extensive region of stratiform precipitation was sampled north of the storm circulation for several hours before the storm center made landfall.

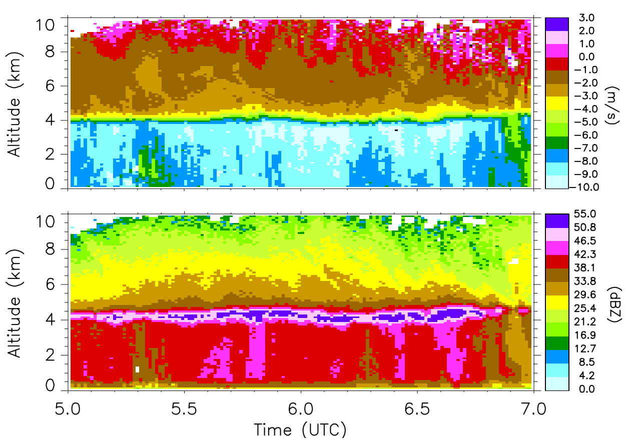

Figure 2. The time-height sections of the Doppler air velocity (top) and reflectivity (bottom) from the 915-MHz profiler on 14 Sep 2001.

The 0600 UTC Tampa Bay sounding indicated the height of the 0° C isotherm near 4.7 km. The level of the bright band undulated slightly from 0500 to 0650 UTC. During this time, the reflectivity profiles showed slightly increasing or uniform values with decreasing height below the melting layer and showed some bulges over several kilometers above the strong bright band, which is related to active aggregation of snow particles. The rainfall rates showed an increase up to 15~20 $mmhr^{-1}$ through 0600 to 0650 UTC as the depth of the bright band became wider and stronger. During this period, wind fields were sufficiently uniform to meet the assumption for the EVAD technique.

In Figure 3, the horizontal divergence from EVAD is compared to that calculated from the 915-MHz profiler measurements. The divergence and vertical air motion profiles derived from the 915-MHz profiler were averaged out over the 5 min radar sampling period of an entire volume scan. The 915-MHz divergence was calculated using u and v components of the wind and then was density-weighted for the interval of each gate spacing. In the figure, the wind profiler divergence induced by precipitation-driven downdrafts exists near the surface. Divergence and convergence features relatively match well with those of the scanning radar above the melting layer up to 10 km. The 915-MHz profiler shows much larger magnitudes of divergence and convergence compared to those of the scanning radar. There exists weak convergence in the vicinity of melting layer and divergence peak just below it. This couplet of convergence and divergence might be due to the small-scale inflows and outflows driving descents or ascents in the melting layer. However, the SMART-Radar shows weak or near zero divergence around the melting layer. The discrepancy results from the fact that the sampling area of the wind profiler is much smaller than that of the scanning radar. The scanning radar is designed to analyze the mesoscale air flows so that it is hard to resolve small-scale changes in the wind. The vertical air motion from EVAD shows the mesoscale upper-level ascent which is typical of the stratiform regions of mesoscale convective systems, crossing over at 7 km altitude in Figure 3. The vertical air motion from the 915-MHz profiler was negatively biased downward to the surface, which may be due to an inappropriate top boundary condition. According to the cloud-top temperature from the infrared satellite imagery, the cloud top of this system was near 14 km. Incorrect values of divergence at the echo top of 10 km also may result in this bias and error as integrated downward. The biases in vertical air motion estimates below the melting layer are possibly from the increased target fall speeds. Cifelli et al

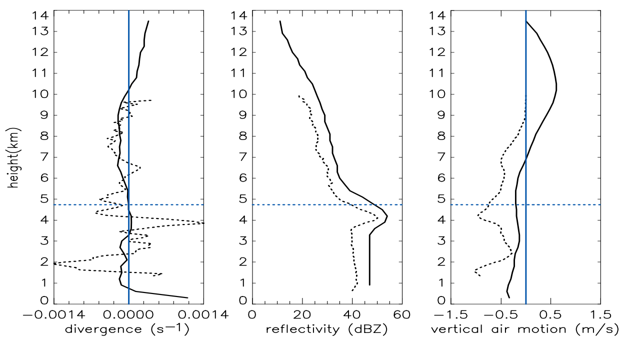

Figure 3. The profiles of horizontal divergence(left), reflectivity(middle), and vertical air motion(right) on 0602 UTC obtained from EVAD (black thick line) and the 915-MHz profiler(dotted line).

(1996) indicated that the errors of divergence and vertical air motion, especially in the vicinity of the melting layer of the wind profiler, result from many sources including precipitation contamination, divergence field evolution during the sampling period, or an inappropriate top boundary condition. The 915-derived reflectivities are in good agreement with the SMART-Radar reflectivities when the 7 dB bias is removed. The bright band region of the SMART-Radar reflectivities is much wider and smoother, compared to that of the 915-MHz profiler since the SMART-Radar reflectivities are averaged values over horizontal rings included in elevation cones of each layer.

5. DROP SIZE DISTRIBUTIONS

Vertical air motions from the EVAD analysis will be used as complementary information on the retrieval of drop size distributions using the Sans Air Motion (SAM) model (Williams 2002). In this model, the clear air spectrum is separated from the measured Doppler spectrum to get the hydrometeor spectrum that produces the raindrop size distribution. In deriving ice size distributions, it is important to estimate correct terminal fall speeds of ice particles because their fall speeds at 1~2 ms^{-1} are much smaller than those of rain drops and directly correspond to sizes of ice crystals, providing information on their types. We will use the terminal fall speeds from the EVAD analysis for examining ice sizes and distributions using the Doppler spectrum measured by the 915-MHz profiler in conjunction with the SAM model.

6. CONCLUSIONS

The horizontal divergence and vertical air motion profiles obtained through the EVAD method and the 915-MHz profiler measurements were examined for the widespread stratiform region of the landfalling storm. There existed some discrepancies in horizontal divergence and vertical air motion due to the large difference in spatial and temporal scales between the SMART-Radar and the 915-MHz profiler. The 915-MHz profiler convergence and divergence features were qualitatively coincident with those from SMART-Radar. The relatively strong wind shears or the beam blockages found at low elevation angels affected the estimates of divergence near the surface. The wind profiler showed some biases and errors in vertical air motion estimates because of the high variations of the wind fields in the melting layer and near the surface. The inappropriate top boundary condition also contributed to the biased vertical air motions. In the future, the vertical motion and terminal fall speed profiles obtained by these two techniques are used to refine the retrieval of drop size distributions derived from Doppler spectra below the melting level, and ice particle size distributions above the melting level.

7. REFERENCES

Browning, K. A., and R. Wexler. 1968: The Determination of Kinematic Properties of a Wind Field Using Doppler Radar. *Journal of Applied Meteorology.,* 7, 105–113.

Cifelli, R., S. A. Rutledge, D. J. Boccippio and T. Matejka. 1996: Horizontal Divergence and Vertical Velocity Retrievals from Doppler Radar and Wind Profiler Observations. *Journal of Atmospheric and Oceanic Technology.,* **13,** 948–966.

Matejka, T., and R. C. Srivastava. 1991: An Improved Version of the Extended Velocity-Azimuth Display Analysis of Single-Doppler Radar Data. *Journal of Atmospheric and Oceanic Technology.,* **8,** 453–466.

Srivastava, R. C., T.J. Matejka and T.J. Lorello. 1986: Doppler Radar Study of the Trailing Anvil Region Associated with a Squall Line. *Journal of the Atmospheric Sciences.,* **43,** 356–377.

Williams, C. R., 2002: Simultaneous ambient air motion and raindrop size distributions retrieved from UHF vertical incident profiler observations., *Radio Sci.,* **37,** 1024